

Optical properties of elongated conducting grains

X.M. Huang^{1,2}, Qi Li^{3,2*}, Aigen Li^{2†}, J.H. Chen^{1,2‡}, F.Z. Liu^{4,2}, and C.Y. Xiao⁵

¹College of Physics and Electronics, Hunan Normal University, Changsha, Hunan 410081, China

²Department of Physics and Astronomy, University of Missouri, Columbia, MO 65211, USA

³Hunan Key Laboratory for Stellar and Interstellar Physics and School of Physics and Optoelectronics, Xiangtan University, Hunan 411105, China

⁴College of Information Science and Engineering, Hunan Normal University, Changsha, Hunan 410081, China

⁵Department of Astronomy, Beijing Normal University, Beijing 100875, China

ABSTRACT

Extremely elongated, conducting dust particles (also known as metallic “needles” or “whiskers”) are seen in carbonaceous chondrites and in samples brought back from the Itokawa asteroid. Their formation in protostellar nebulae and subsequent injection into the interstellar medium have been demonstrated, both experimentally and theoretically. Metallic needles have been suggested to explain a wide variety of astrophysical phenomena, ranging from the mid-infrared interstellar extinction at $\sim 3\text{--}8\ \mu\text{m}$ to the thermalization of starlight to generate the cosmic microwave background. To validate (or invalidate) these suggestions, an accurate knowledge of the optics (e.g., the amplitude and the wavelength dependence of the absorption cross sections) of metallic needles is crucial. Here we calculate the absorption cross sections of iron needles of various aspect ratios over a wide wavelength range, by exploiting the discrete dipole approximation, the most powerful technique for rigorously calculating the optics of irregular or nonspherical grains. Our calculations support the earlier findings that the antenna theory and the Rayleigh approximation, which are often taken to approximate the optical properties of metallic needles, are indeed inapplicable.

Key words: dust, extinction – infrared: ISM – intergalactic medium

1 INTRODUCTION

Extremely elongated, needle- or whisker-like metallic grains are long known to be present in extraterrestrial environments. Bradley et al. (1996) performed an analytical transmission electron microscopic examination of the Martian meteorite ALH84001 and reported the detection of nano-sized magnetite (Fe_3O_4) whiskers and platelets in association with carbonates in fracture zones within ALH84001. Based on Raman imaging and electron microscopy, Fries & Steel (2008) discovered graphite whiskers in three CV-type carbonaceous chondrites. They found that the graphite whiskers are associated with high-temperature calcium-aluminum inclusion rims and interiors. Steele et al. (2010) conducted two- and three-dimensional confocal Raman imaging spectroscopy of an Apollo 17 impact melt breccia and found micron-sized graphite, rolled-graphene sheets and graphite whiskers, probably resulting from the impact processes responsible for breccia formation. More recently, Matsumoto et al. (2020) obtained high-resolution transmission

electron microscopic images of the dust particles returned by the Japanese Hayabusa mission to the Itokawa asteroid and reported the discovery of iron whiskers on asteroidal particles.

Nuth et al. (2010) have experimentally shown that abundant graphite whiskers could be formed on or from the surfaces of graphite grains if they are repeatedly exposed to H_2 , CO , and N_2 at 875 K, a condition mimicing that of protostellar nebulae. These newly formed graphite whiskers could subsequently be expelled from protostellar systems either in polar jets or by radiation pressure and populate the interstellar space (Bland 2008, Nuth et al. 2010). Hoyle & Wickramasinghe (1988) suggested that metallic whiskers could form efficiently in supernova ejecta through screw dislocation. Piotrowski (1962) argued that electrically charged interstellar grains, if elongated, tend to grow longer in the interstellar medium (ISM) through preferential capture of ions near the ends of the grain. In addition, Nuth et al. (1994), Nuth & Wilkinson (1995) and Marshall et al. (2005) have shown both experimentally and theoretically that the nano-sized iron grains in the solar nebula could grow to whiskers with an almost infinite length-to-diameter ratio at greatly enhanced rates due to the electrostatic and magnetic dipole interactions.

* qili@xtu.edu.cn

† lia@missouri.edu

‡ jhchen@hunnu.edu.cn

Metallic whiskers or needles have unique, elongation-dependent optical properties. Because of this, they have been invoked to explain a wide variety of astrophysical phenomena. Exceedingly elongated metallic needles, presumably present in the intergalactic medium (IGM), have been suggested as a source of starlight opacity to thermalize starlight in a steady-state cosmology to create a non-cosmological microwave background (Hoyle & Wickramasinghe 1988), as well as to explain the microwave background anisotropy (Narlikar et al. 2003) detected by the Wilkinson Microwave Anisotropy Probe (Bennett et al. 2003). Such needles have also been investigated by Wright (1982) and Aguirre (2000) as a thermalizing agent of starlight to generate a cold big bang microwave background. Aguirre (1999) and Banerjee et al. (2000) have also explored the possibilities of needles as a source of the gray opacity needed to account for the observed redshift-magnitude relation of Type Ia supernovae (Riess et al. 1998; Perlmutter et al. 1999) without resorting to a positive cosmological constant. More recently, Melia (2020, 2021) has thoroughly examined the possible rethermalization of the cosmological microwave background photons by dust ejected into the intergalactic medium by the first-generation Population III stars at redshift $z < 16$. In addition, metallic needles have been suggested by Dwek (2004a) and explored also by Wang et al. (2014) as an explanation for the anomalously flat mid infrared (IR) interstellar extinction at $\sim 3\text{--}8\ \mu\text{m}$ seen in both diffuse and dense environments (Lutz 1999, Indebetouw et al. 2005, Jiang et al. 2006, Flaherty et al. 2007, Gao et al. 2009, Nishiyama et al. 2009, Wang et al. 2013, Xue et al. 2016, Hensley & Draine 2020), in stark contrast to the deep minimum expected from standard interstellar dust models (see Draine 1989, Weingartner & Draine 2001). Metallic needles have also been suggested by Dwek (2004b) as the source for the submillimeter excess observed by Dunne et al. (2003) along the line of sight toward the Cas A supernova remnant (but also see Krause et al. 2004, Wilson & Batrla 2005, Gomez et al. 2005, 2009).

The ascription of the aforementioned astrophysical phenomena to metallic needles is largely based on their conceived unique, anomalously large opacities over a wide range of wavelengths from the ultraviolet (UV) all the way to the IR, submillimeter and millimeter, with the wavelength span depending on their geometrical (e.g., the length over radius ratio) and physical (e.g., the resistivity) properties. Unfortunately, there lacks exact solution to the scattering and absorption of light with metallic needles. In the literature, the absorption cross sections of metallic needles are often derived either from extremely elongated spheroids under the Rayleigh approximation (see Li 2003 and references therein) or from the antenna approximation (see Xiao et al. 2020 and references therein). However, it has been shown that, for highly conducting needles, the Rayleigh criterion is not satisfied and therefore the Rayleigh approximation is invalid (see Li 2003). On the other hand, very recently it has also been shown that the antenna approximation is not an appropriate representation for the absorption cross sections of metallic needles since it violates the Kramers-Kronig relation (see Xiao et al. 2020).

In this work we aim at calculating the absorption and scattering cross sections of metallic needles of various elongations over a wide wavelength range from the far-UV to

the mid-IR by employing the discrete dipole approximation (DDA; Purcell & Pennypacker 1973, Draine 1988), a powerful technique known to be capable of accurately calculate the optical properties of nonspherical or irregular particles. In §2 we briefly present the computational method and targets. The results are presented and discussed in §3. Our major conclusion is summarized in §4.

2 THE COMPUTATIONAL METHOD

The DDA method, also known as the coupled dipole approximation, is a powerful numerical technique for calculating the scattering and absorption of electromagnetic radiation by dust particles of arbitrary geometry. This method divides a targeted dust particle into a discrete set of interacting dipoles on a cubic lattice in which the dipoles are separated by a distance d . The dipoles, whose properties are defined by the dielectric properties of the dust material, can be distributed inside the cubic array without restrictions and thus, as long as the inter-dipole lattice spacing d is small enough, the geometry of any arbitrarily shaped dust particles can be adequately simulated. In the cubic array, each dipole responds to the incident electric field as well as the fields contributed by all other dipoles. The collective responses of all these dipoles allow for the scattering and absorption properties of dust particles of any geometric shape and composition to be accurately calculated, provided that the condition $|m|kd < 1$ is satisfied, where m is the complex refractive index, $k = 2\pi/\lambda$ is the wave number, and λ is the wavelength (see Draine & Flatau 2013). Due to its versatility and accuracy, the DDA method has been widely used to simulate the optical responses of nonspherical dust particles.

We perform DDA calculations for elongated conducting grains by using the DDSCAT7.3 software package (Draine & Flatau 2013). These grains are represented by circular cylinders of radius a , length l , mass density ρ_m , and mass $m_{\text{dust}} = \pi a^2 l \rho_m$. The volume-equivalent sphere radius—the radius of a sphere having the same volume as the cylindrical grain is $a_{\text{eff}} = (3a^2 l/4)^{1/3}$. We consider iron grains since iron needles have been invoked to explain a variety of astrophysical phenomena and there is increasing evidence for the depletion of Fe in iron grains, not in silicate dust (see Xiao et al. 2020).

3 RESULTS AND DISCUSSION

We consider circular cylindrical iron grains of five different radii $a = 0.001, 0.003, 0.01, 0.03, 0.1\ \mu\text{m}$. For grains with a given radius, five different elongations (or aspect ratios) of $l/a = 2, 5, 10, 30, 100$ are considered. The wavelength-dependent indices of refraction of iron are taken from Li (2003). We consider 52 different wavelengths equally spaced on a logarithmic scale and ranging from $0.1\ \mu\text{m}$ to $17\ \mu\text{m}$. These wavelengths cover the far-UV to the mid-IR range which is relevant to the optical diagnostic of starlight extinction and heating by iron grains in the ISM. Ideally, it would be desirable if larger grains (up to several submicrons), larger elongations (up to $\sim 10^4$), and longer wavelengths (up to millimeters) can be considered. However,

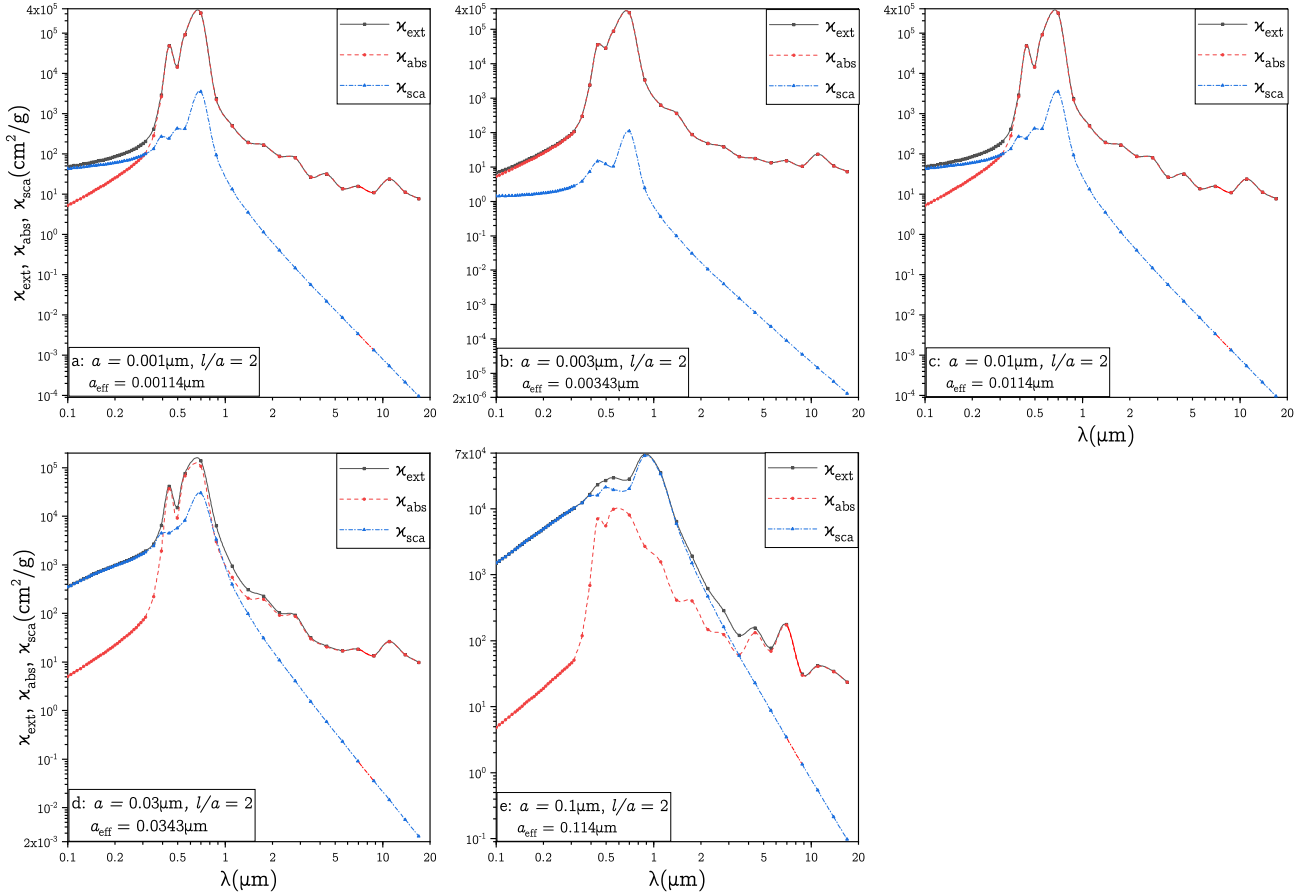


Figure 1. Extinction (black solid lines), absorption (red dashed lines), and scattering (blue dot-dashed lines) mass coefficients of circular cylindrical iron grains of an elongation $l/a = 2$ and radii $a = 0.001 \mu\text{m}$ (a), $0.003 \mu\text{m}$ (b), $0.01 \mu\text{m}$ (c), $0.03 \mu\text{m}$ (d), and $0.1 \mu\text{m}$ (e).

in order to meet the criterion of $|m|kd < 1$ required for DDSCAT7.3 to be accurate, the number of dipoles used to represent such grains would considerably exceed 10^6 so that the inter-dipole distance d would not exceed $\lambda / (2\pi|m|)$.¹ This poses a severe challenge on computational demand and makes it impractical.

Let $C_{\text{ext}}(a, l, \lambda)$, $C_{\text{abs}}(a, l, \lambda)$, and $C_{\text{sca}}(a, l, \lambda)$ respectively be the extinction, absorption and scattering cross sections of a circular iron cylinder of radius a and length l at wavelength λ . The extinction, absorption and scattering mass coefficients of such a grains are $\kappa_{\text{ext}}(a, l, \lambda) \equiv C_{\text{ext}}(a, l, \lambda) / (\pi a^2 l \rho_m)$, $\kappa_{\text{abs}}(a, l, \lambda) \equiv C_{\text{abs}}(a, l, \lambda) / (\pi a^2 l \rho_m)$, and $\kappa_{\text{sca}}(a, l, \lambda) \equiv C_{\text{sca}}(a, l, \lambda) / (\pi a^2 l \rho_m)$, respectively.

In Figure 1 we show the extinction, absorption and scattering mass coefficients of iron cylinders of $a = 0.001, 0.003, 0.01, 0.03, 0.1 \mu\text{m}$ and $l/a = 2$. Most pronounced in the extinction mass coefficient profiles is a broad bump lying in the wavelength range of $\sim 0.3\text{--}1 \mu\text{m}$. This broad bump exhibits two resonant peaks at ~ 0.44 and $\sim 0.70 \mu\text{m}$. These extinction peaks arise from resonances in

the collective motion of free electrons constrained to oscillate within small grains (Bohren & Huffman 1983).

For grains of $a \lesssim 0.03 \mu\text{m}$, the extinction is predominantly contributed by absorption, while scattering is negligible. As grain size increases, scattering becomes important and surpasses absorption for grains with $a = 0.1 \mu\text{m}$. This is probably due to the so-called “skin depth” effect, i.e., only a small fraction of the incident light can “get into” the grain to be absorbed and no appreciable light penetrates through the grain (Bohren & Huffman 1983). Also, the extinction bump is considerably broadened for grains with $a = 0.1 \mu\text{m}$ at the expense of its height.

Similarly, we show in Figures 2–5 the extinction, absorption and scattering mass coefficients of iron cylinders of $l/a = 5, 10, 30, 100$. Again, for each elongation l/a , we consider grains of five different radii $a = 0.001, 0.003, 0.01, 0.03, 0.1 \mu\text{m}$. Compared with grains of an elongation $l/a = 2$ (see Figure 1), more elongated grains with the same radii generally tend to exhibit more prominent resonant structures in their extinction profiles. These resonant structures are appreciably broadened and span a wider wavelength range in grains with larger elongations and larger radii. Most notably, the sharp extinction peaks which are prominent in grains of $l/a = 100$ and $a \lesssim 0.03 \mu\text{m}$ fade away in grains of $l/a = 100$ and $a = 0.1 \mu\text{m}$.

¹ Note that for conducting materials like iron, the index of refraction m increases with wavelength (see Li 2003) and the required number of dipoles would be even larger at longer wavelengths.

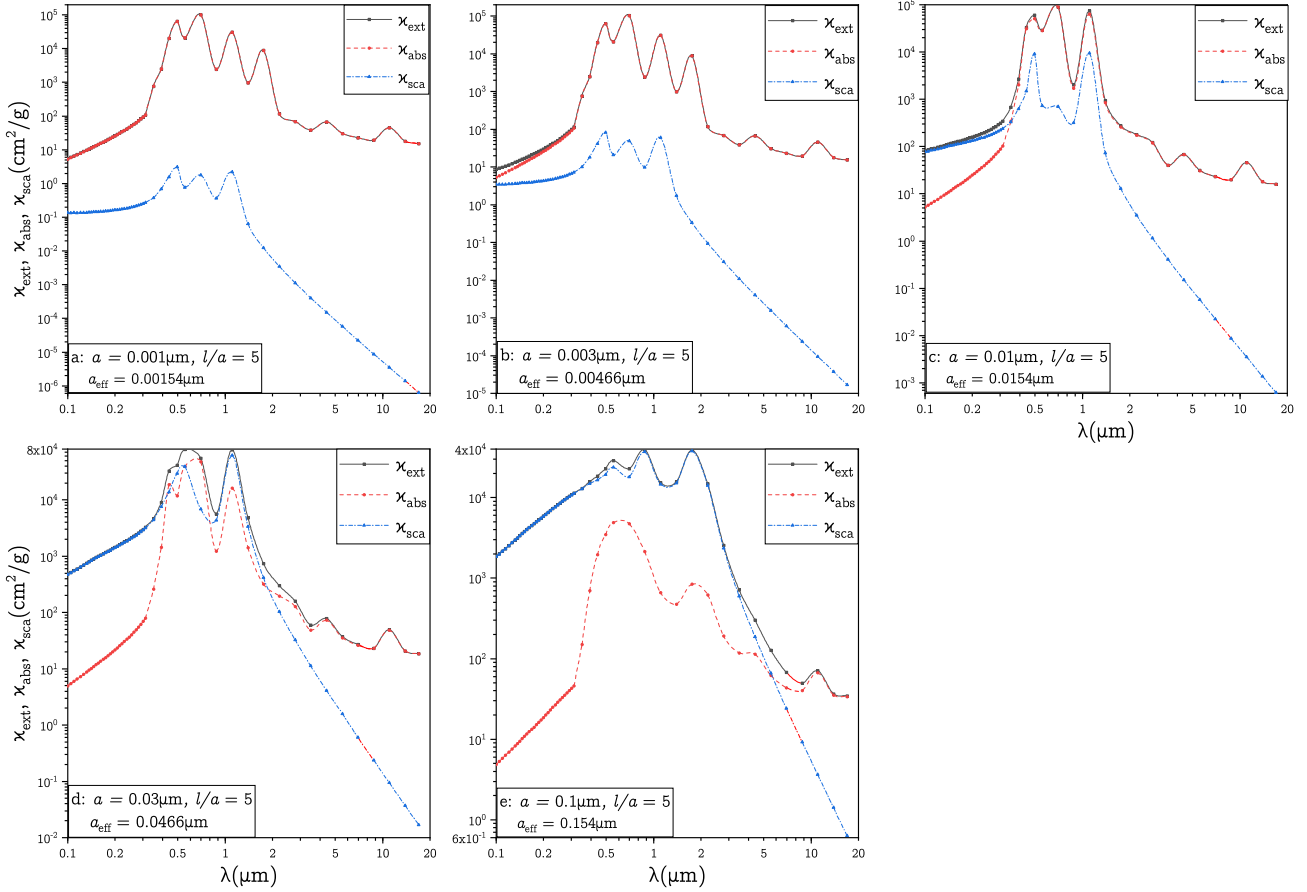


Figure 2. Same as Figure 1 but for iron grains of an elongation $l/a = 5$.

For highly elongated needle-like conducting grains, Rayleigh approximation is often employed to estimate their extinction properties (see Li 2003 and references therein):

$$\kappa_{\text{ext}}(a, l, \lambda) = \left(\frac{4\pi}{3c\rho_m\rho_R} \right) \left(\frac{1}{1 + (\lambda/\lambda_0)^2} \right), \quad (1)$$

where c is the speed of light, ρ_R the dust resistivity, and λ_0 , the long-wavelength cutoff, is estimated from

$$\lambda_0 \approx \frac{c\rho_R}{2} \frac{(l/a)^2}{\ln(l/a)}. \quad (2)$$

It is seen that eq.(2) establishes a lower bound on the elongation l/a of the needles which absorb strongly at wavelengths out to λ_0 .

We have also calculated the extinction mass coefficients for iron cylinders of $l/a = 100$ and $a = 0.001, 0.003, 0.01, 0.03, 0.1 \mu\text{m}$ by making use of the Rayleigh approximation. As shown in Figure 5, it is obvious at a glance that the extinction mass coefficients derived from the Rayleigh approximation are totally different from that calculated from DDSCAT7.3 which is believed to be accurate. This demonstrates that the Rayleigh approximation is not valid for iron needles. Indeed, Li (2003) has shown that the Rayleigh approximation is not applicable to conducting needles since the Rayleigh criterion is not satisfied.

Similarly, conducting needles are often also approximated as antennae and their extinction properties are es-

timated from the antenna theory (see Xiao et al. 2020 and references therein):

$$\kappa_{\text{ext}}(a, l, \lambda) = \left(\frac{4\pi}{3c\rho_m\rho_R} \right), \quad \lambda \leq \lambda_0, \quad (3)$$

$$= \left(\frac{4\pi}{3c\rho_m\rho_R} \right) \left(\frac{\lambda}{\lambda_0} \right)^{-2}, \quad \lambda > \lambda_0, \quad (4)$$

where the long-wavelength cutoff λ_0 is estimated from eq.2.

We have also calculated the extinction mass coefficients for iron cylinders of $l/a = 100$ and $a = 0.001, 0.003, 0.01, 0.03, 0.1 \mu\text{m}$ by making use of the antenna theory. The results, as shown in Figure 5, are close to that of the Rayleigh approximation, but markedly differ from those computed from DDSCAT7.3, not only in the extinction magnitudes but also in the extinction spectral shapes. Evidently, neither the Rayleigh approximation nor the antenna theory can account for the resonant structures that are conspicuous in the extinction profiles calculated from DDSCAT7.3. Although considerably squelched, they are still perceptible in the extinction profile of grains of $l/a = 100$ and $a = 0.1 \mu\text{m}$. Therefore, like Rayleigh approximation, the antenna theory is not an appropriate representation for the extinction properties of metallic needles. As a matter of fact, Xiao et al. (2020) have shown that the antenna approximation violates the Kramers-Kronig relation.

It is interesting to note that, as mentioned earlier, the

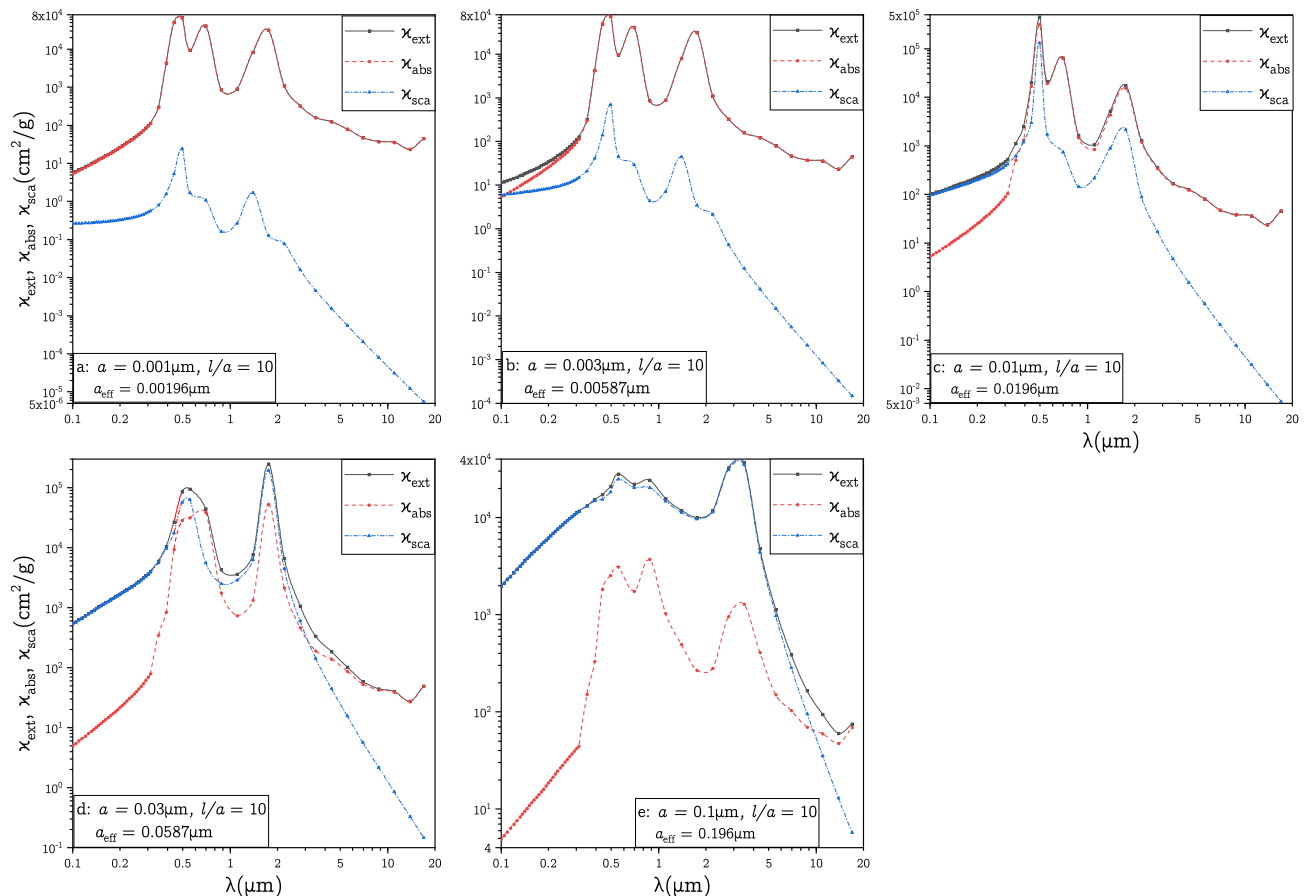


Figure 3. Same as Figure 1 but for iron grains of an elongation $l/a = 10$.

resonant structures are notably damped in the extinction profiles of grains of larger radii and larger elongations (e.g., see Figure 5 for $l/a = 100$ and $a = 0.1 \mu\text{m}$), although far less smooth than those derived from the antenna theory and the Rayleigh approximation. Such grains could provide the “gray” opacity to explain the flat mid-IR extinction at $\sim 3\text{--}8 \mu\text{m}$ seen in various interstellar regions. A rough estimate suggests that iron needles of $l/a = 100$ and $a = 0.1 \mu\text{m}$, with $\text{Fe}/\text{H} \sim 20$ ppm, are capable of accounting for the observed mid-IR extinction.

Finally, we also note that the resonant spectral features seen in the extinction profiles of elongated, individual grains are unlikely present in the ISM. First of all, metallic needles, if indeed present in the ISM, would likely consist of a distribution of radii and elongations. It is unlikely that they are just a string of identically-sized grains in a perfectly straight line of the same length. While individual grains exhibit resonant structures in their extinction profiles which are specific to their radii and lengths, these fine structures will be smoothed out if a distribution of grain sizes are incorporated into a distribution of chain lengths (see §11.3.2 in Bohren & Huffman 1983) that would be more likely to represent the actual grains in the ISM. Also, actual conducting grains in the ISM are unlikely as perfectly straight as graphite needles or rolled graphene sheets (e.g., see Kimura & Kaito 2008, Silva et al. 2021). In fact, images of experimentally-grown grain

aggregates (grown either magnetically or electrostatically) display a wide range in angles between any three adjacent dust grains and are “kinky” at almost every junction (see Nuth et al. 1994, 2010). The spectral resonances seen in individual grains are expected to be cancelled out in such “kinky” aggregates of grains of a range of sizes, chain lengths and inter-grain angles (see Bohren & Huffman 1983).

4 SUMMARY

We have utilized DDA to simulate the interaction of elongated conducting iron grains of various sizes and elongations with electromagnetic waves from the far-UV to the mid-IR. It is found that their extinction profiles exhibit pronounced resonant structures in the optical and near-IR which are attributed to resonances in the collective motion of free electrons constrained to oscillate within small grains. These resonant structures are considerably broadened and eventually fade away, if not totally obliterated, as the grain size and/or elongation increases. The extinction profiles of needle-like iron grains of aspect ratios (i.e., length-to-radius ratios) $\gtrsim 100$ and of radii $a \gtrsim 0.1 \mu\text{m}$ are relatively smooth and flat in the optical, near- and mid-IR and could provide the “gray” opacity for accounting for the flat mid-IR extinction at $\sim 3\text{--}8 \mu\text{m}$ observed in various interstellar regions. It is also shown that the widely-adopted Rayleigh approximation and

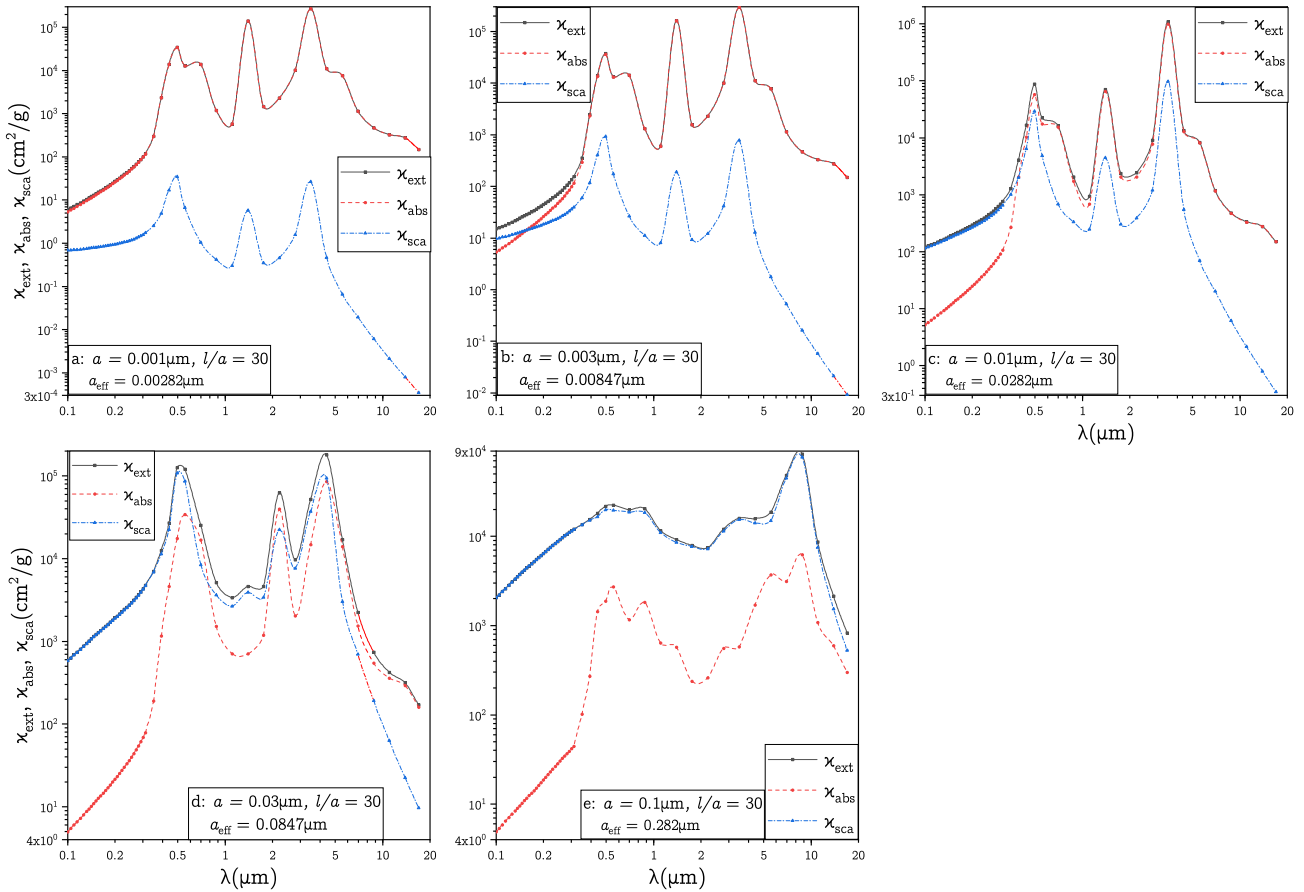


Figure 4. Same as Figure 1 but for iron grains of an elongation $l/a = 30$.

antenna theory do not provide valid representations of the optical properties of highly elongated conducting needle-like grains. Due to the extremely high computational demand of DDA, it is presently rather challenging to calculate the scattering and absorption properties of large conducting grains of high elongations at long wavelengths. We call for experimental measurements of the optical properties of conducting needles of various aspect ratios over a wide wavelength range to bound theoretical calculations.

ACKNOWLEDGEMENTS

We thank Drs. B.T. Draine, E. Dwek, J.A. Nuth III, D. Pfenniger, and J.L. Puget for stimulating discussions and suggestions. JHC and XMH are supported in part by NSFC Grant No. U1731107. AL is supported in part by a NSF grant AST-1816411. CYX is supported in part by the Talents Recruiting Program of Beijing Normal University and the National Natural Science Foundation of China (NSFC) Grant No. 91952111.

DATA AVAILABILITY

The data underlying this article will be shared on reasonable request to the corresponding authors.

REFERENCES

- Aguirre, A.N. 1999, *ApJL*, 512, L19
Aguirre, A.N. 2000, *ApJ*, 533, 1
Banerjee, S.K., Narlikar, J.V., Wickramasinghe, N.C., Hoyle, F., & Burbridge, G. 2000, *AJ*, 119, 2583
Bennett, C.L., et al. 2003, *ApJS*, 148, 1
Bland, P.A. 2008, *Science*, 320, 61
Bohren, C.F., & Huffman, D.R. 1983, *Absorption and Scattering of Light by Small Particles*, Wiley, New York
Bradley, J. P., Harvey, R. P., & McSween, H. Y. 1996, *Geochim. Cosmochim. Acta*, 60, 5149
Draine, B.T. 1988, *ApJ*, 333, 848
Draine, B.T. 1989, in *Infrared Spectroscopy in Astronomy*, ed. B. H. Kaldeich (Paris: ESA Publ. Division), 93
Draine, B.T. & Flatau, P.J. 1994, *J. Opt. Soc. Am. A*, 11, 1491.
Draine, B.T. & Flatau, P.J. 2013, arXiv:1305.6497
Dunne, L., Eales, S., Ivison, R., Morgan, H., & Edmunds, M. 2003, *Nature*, 424, 285
Dwek, E. 2004a, *ApJ*, 611, L109
Dwek, E. 2004b, *ApJ*, 607, 848
Flaherty, K. M., Pipher, J. L., Megeath, S. T., et al. 2007, *ApJ*, 663, 1069
Fries, M. & Steele, A. 2008, *Science*, 320, 91
Gao, J., Jiang, B.W., & Li, A. 2009, *ApJ*, 707, 89
Gomez, H. L., Dunne, L., Eales, S. A., et al. 2005, *MNRAS*, 361, 1012
Gomez, H. L., Dunne, L., Ivison, R. J., et al. 2009, *MNRAS*, 397, 1621

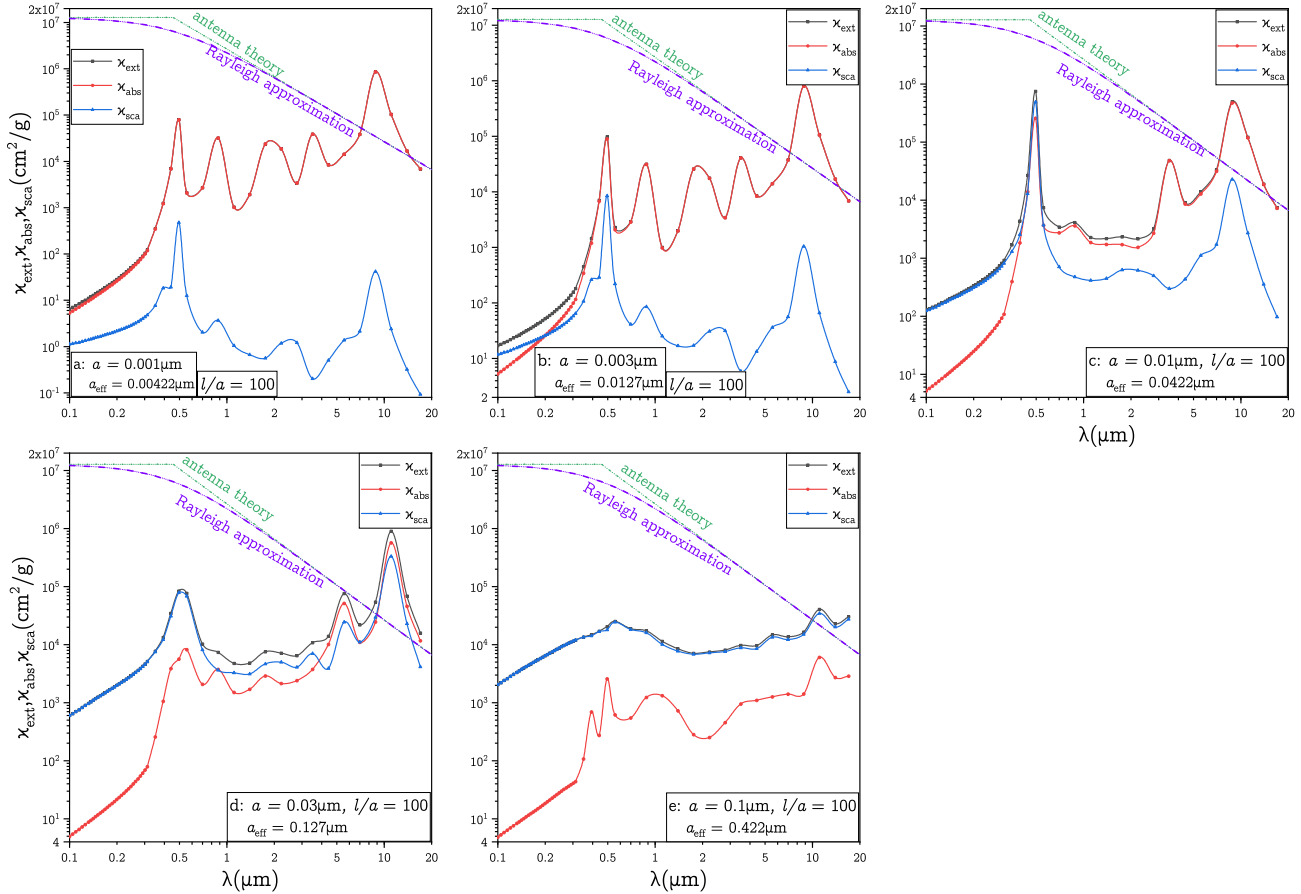


Figure 5. Same as Figure 1 but for iron grains of an elongation $l/a = 100$. Also shown are the extinction mass coefficients derived from the Rayleigh approximation (purple dot-dot-dashed lines) and antenna theory (green dotted lines).

Indebetouw, R., Mathis, J. S., Babler, B. L., et al. 2005, *ApJ*, 619, 931
 Hensley, B. S. & Draine, B. T. 2020, *ApJ*, 895, 38
 Hoyle, F., & Wickramasinghe, N.C. 1988, *Ap&SS*, 147, 245
 Jiang, B.W., Gao, J., Omont, A., Schuller, F., & Simon, G. 2006, *A&A*, 446, 551
 Kimura, Y., & Kaito, C. 2008, *ApJ*, 685, L83
 Krause, O., Birkmann, S.M., Rieke, G.H., et al. 2004, *Nature*, 432, 596
 Li, A. 2003, *ApJ*, 584, 593
 Lutz, D. 1999, in *The Universe as Seen by ISO*, ed. P. Cox & M. Kessler (ESA Special Publ., Vol. 427; Noordwijk: ESA), 623
 Marshall, J. R., Sauke, T. B., & Cuzzi, J. N. 2005, *Geophys. Res. Lett.*, 32, L11202
 Matsumoto, T., Harries, D., Langenhorst, F., et al. 2020, *Nature Comm.*, 11, 1117
 Melia, F. 2020, *European Phys. J. Plus*, 135, 511
 Melia, F. 2021, *European Phys. J. Plus*, in press (arXiv:2103.04241)
 Narlikar, J.V., Vishwakarma, R.G., Hajian, A., Souradeep, T., Burbidge, G., & Hoyle, F. 2003, *ApJ*, 585, 1
 Nishiyama, S., Tamura, M., Hatano, H., et al. 2009, *ApJ*, 696, 1407
 Nuth, J. A. & Wilkinson, G. M. 1995, *Icarus*, 117, 431
 Nuth, J. A., Berg, O., Faris, J., & Wasilewski, P. 1994, *Icarus*, 107, 155
 Nuth, J. A., Kimura, Y., Lucas, C., et al. 2010, *ApJL*, 710, L98
 Perlmutter, S., et al. 1999, *ApJ*, 517, 565

Piotrowski, S.L. 1962, *Acta Astron.*, 12, 221
 Purcell, E. M., & Pennypacker, C. R. 1973, *ApJ*, 186, 705
 Riess, A. G., et al. 1998, *AJ*, 116, 1009
 Silva, C., Chrostoski, P., & Fraundorf, P. 2021, *MRS Advances* (<https://doi.org/10.1557/s43580-021-00022-3>)
 Steele, A., McCubbin, F.M., Fries, M., et al. 2010, *Science*, 329, 51
 Wang, S., Gao, J., Jiang, B.W., Li, A., & Chen, Y. 2013, *ApJ*, 773, 30
 Wang, S., Li, A., & Jiang, B.W. 2014, *Planet. Space Sci.*, 100, 32
 Weingartner, J.C., & Draine, B.T. 2001, *ApJ*, 548, 296
 Wilson, T. L., & Batrla, W. 2005, *A&A*, 430, 561
 Wright, E.L. 1982, *ApJ*, 255, 401
 Xiao, C.Y., Li, Q., Li, A., & Chen, J.H. 2020, *MNRAS*, 498, 3560
 Xue, M., Jiang, B.W., Gao, J., Liu, J.M., Wang, S., & Li, A. 2016, *ApJS*, 224, 23

This paper has been typeset from a \TeX / \LaTeX file prepared by the author.